



# Analysis of Chip Formation and Temperature Measurement in Machining of Titanium Alloy (Ti-6Al-4V)

Ramesh S<sup>1</sup> · K. Palanikumar<sup>2</sup> · S.B. Boppana<sup>3</sup> · E. Natarajan<sup>4</sup>

Received: 25 July 2021 / Accepted: 10 December 2021 / Published online: 31 January 2022  
© The Society for Experimental Mechanics, Inc 2022

## Abstract

This research investigates the cutting zone temperature while machining Titanium alloy (Ti-6Al-4 V), as Ti64 happens to be the most important material utilized in building aircraft, dental implants and jet engines. This alloy is the low thermal conductivity material which develops high temperature build up in material during machining. The elevated cutting zone temperature affects surface integrity and tool life of the material. These are mainly influenced by machining parameters for instance, feed rate ( $f$ ), depth of cut ( $d$ ) and cutting speed ( $v$ ). Thermal images depicting the temperature build up zone were captured using thermal imaging camera during machining. Experimental investigations reveals that the cutting temperature has increasing trend with cutting speed. The machining model was done based on experimental outputs using Response Surface Methodology (RSM) technique. The response of the developed model was mapped within the range of the cutting conditions. The optimal combination of machining parameters was evaluated to minimize temperature. PVD carbide tool and CVD coated tools performance are almost similar. CVD coated tools produces short chips during machining whereas PVD coated tool produces comparatively long chips.

**Keywords** Titanium alloy · Temperature · Thermal image · Machining · Response surface methodology · Coated carbide insert · Orthogonal array

## Introduction

Titanium alloy is one of the strongest metals which is mostly used in automobile, railway, ship building, aircraft manufacture and construction industries. Titanium alloy has a low thermal conductivity and high weldability [1, 2]. Titanium alloys are related to metals that predominantly consisting of titanium (Ti) and supplementary chemical elements like aluminium and vanadium [3, 4]. They offer high toughness and tensile strength even at the critical temperature or elevated temperature. They are lightweight materials that can

exhibit higher resistance to corrosion and are able to withstand higher temperatures. Titanium alloy (Ti64) is typically alloyed with calculated amount of aluminium and vanadium, usually with a weight percentage of 6 and 4 respectively [5]. The incorporation of these elements increases not only the strength but also the plasticity. The conventional tools wear out rapidly when employed in machining of Ti alloy continuously. Tool materials like cemented carbide and ceramics are usually found to be susceptible with Ti alloy at higher temperatures [6, 7].

The temperature attained during cutting will have immense effect on the tool life and surface integrity of the material being machined. The yield strength is also found to decrease with the increasing temperature during cutting. The increase in temperature is due to transformation of cutting energy into heat [8, 9]. The heat liberated at the zone of cutting is found to be a prominent factor in deciding the performance of the tool. This is also related to the quality of the surface finish. When the temperature generated due to cutting is sufficiently high, it is found to be unfavourable to the work piece as well as tool. The low cutting temperature may be useful in improving the tool life.

✉ K. Palanikumar  
palanikumar@sairamit.edu.in

<sup>1</sup> Department of Mechanical Engineering, Jerusalam College of Engineering, Chennai, India  
<sup>2</sup> Department of Mechanical Engineering, Sri Sairam Institute of Technology, Chennai, India  
<sup>3</sup> Department of Mechanical Engineering, Presidency University, Bengaluru, India  
<sup>4</sup> Faculty of Engineering, Technology and Built Environment, UCSI University, Kuala Lumpur, Malaysia



Abhang et al. [1] estimated the temperature at the chip-tool interface during turning operation. They investigated cutting parameters such as cutting speed ( $v$ ), feed rate ( $f$ ), depth of cut ( $d$ ) and tool nose radius and reported that increase in speed, feed and depth of cut activates the temperature rise, while nose radius reduces the increase of temperature. Grzesik et al. [10] used thermocouples (K-type) to assess temperature during cutting of steel and reported that the temperature is found to be a decisive factor in surface integrity. Ghani et al. [11] investigated the fraction of heat being transformed to the tool at conventional speed as well as high speed and reported that undue increase in temperature rigorously affects the quality of the work piece and tool life. Petter Hagqvist et al. [12] adopted narrow bandwidth spot radiation pyrometer to estimate high temperature at cutting of titanium-based alloy. This method utilizes the spectral emissivity in estimating the temperature.

Heigel et al. [13] estimated the temperature at tool-chip contact zone using infrared sensor. Infrared camera was utilized to record dispersal of temperature, chip curl and rupture during machining. From their investigations at the cutting speed ( $v$ ) ranges from 20 to 100 m/min, they found that 6–21% of variance in dissemination of temperature from one edge of the chip to the other, signifying that attention must be paid while executing thermographic calculations at the cutting zone. Machado et al. [14] explored machining of titanium alloy (Ti64) using tungsten carbide insert K10 and reported in their review article that the temperature is about 1000 K even at velocities which are relatively lower than 1 m/s and it shoots up to 1350 K for a speed of 3.33 m/s. The temperatures are usually around 250 K greater than the temperature whilst working with carbon steel. It is also reported that low cutting force is produced at elevated cutting temperatures, which are credited by lesser density and lower thermal conductivity of titanium alloys. The

temperature gradient is indeed much rapid even at lower speeds and hence secondary shear area is associated in the cutting zone. Muller et al. [15] also reported that the absolute temperature is in the range between 1300 and 2000 K while working on titanium alloy. They reported further that temperature distribution at the bottom of the chip is initially seen transient and the later as quasi-stationary. The temperature behaviour at chips is seen asymptotic with growing speed. Though the intensified cutting force at higher speed increases the temperature, the asymptotic behaviour of chips limits the increasing temperature at the cutting zone [16].

Komanduri et al. [17] investigated the mechanism of chip formation and wear at low speed to a moderately high-speed machining of Ti alloys. Turley et al. [18] used high speed camera to observe the chip formation and shearing during machining of Ti alloy and reported that catastrophic shear type chips are formed. Also revealed that greater size of shear strains is found in the shear bands. Friction and associated plastic deformation accelerate the heat at the workpiece-tool interface [19–21]. Ramesh et al. and Viswanathan et al. [22–24], Navneet Khanna and Davim [25] and Kechagias et al. [26] investigated the machinability of different grades of Ti alloys and magnesium alloy using design of experiments (DoE) and statistical method. They were intended to reduce the surface roughness of the machined part. Recently, Akkus et al. [27] utilized statistical methods to optimize the surface roughness, vibration and cutting energy during turning of Ti grade 5 alloy. Aydin et al. [28, 29] investigated the cutting zone temperature and applied finite element modelling (FEM) to analyse the chip formation. In recent research by Aydin [30], chip formation at conventional speed and high-speed machining was reported. It was also reported that saw tooth chips are formed at high-speed machining of Ti alloy due to ductile fracture. Optimization of cutting parameters are generally

**Fig. 1** PVD and CVD coated carbide turning tools



done to increase the surface finish and/or material removal rate [31–33] of the machined component.

The present investigation is intended to explore and evaluate the optimum parameters that influencing turning of Ti64 alloy and to attain the optimum cutting zone temperature to enhance tool life. The extended purpose of this research to improve the surface finish of the component.

### Experiments and Measurement of Temperature

The turning experiments were performed on Titanium alloy (Ti64) with the use of coated carbide inserts. CNC turning lathe (Make: PROTECK, India) and high precision thermal imaging camera were employed in the experiments and measurement of cutting temperature with respect to different cutting conditions. Turning tools used were carbide tools with nose radius of 0.8 mm, namely PVD (CNMG 120408 WS 25 PT) and CVD (CNMG 120408 WS 25 PT).PVD coating is TiN coating, generally done by Physical Vapour Deposition technique. CVD is a Chemical Vapour Deposition which contains the coating materials of TiN, TiC, Ti (CN) and Al<sub>2</sub>O<sub>3</sub>. The PVD and CVD coated carbide tools are shown in Fig. 1 (left and the right side respectively). The composition of titanium alloy obtained from the Optical Emission Spectrometer is listed in Table 1. It evidences Grade 5 Titanium alloy that was being machined.

The material Ti64 is a furnace cooled metal that must have the annealed structure. The structure has elongated grains of bright alpha and inters granular beta structure in black colour. Figure 2 reveals the alpha beta structure of the Grade 5 Titanium alloy, where uniform grain sizes are also evidenced. The uniform grain size is achieved if rate of cooling is statically uniform. The bigger size of grains is appeared if there is a variant rate of cooling. At the higher magnification (200X), beta grains are evidenced between alpha grain boundaries.

Figure 3 shows the experimental setup that was being used for turning of Ti64 alloy and thermal image capturing. Table 2 unveils the specification of CNC lathe used in the experiments. It has a swing diameter of 450 mm and length of 1000 mm.

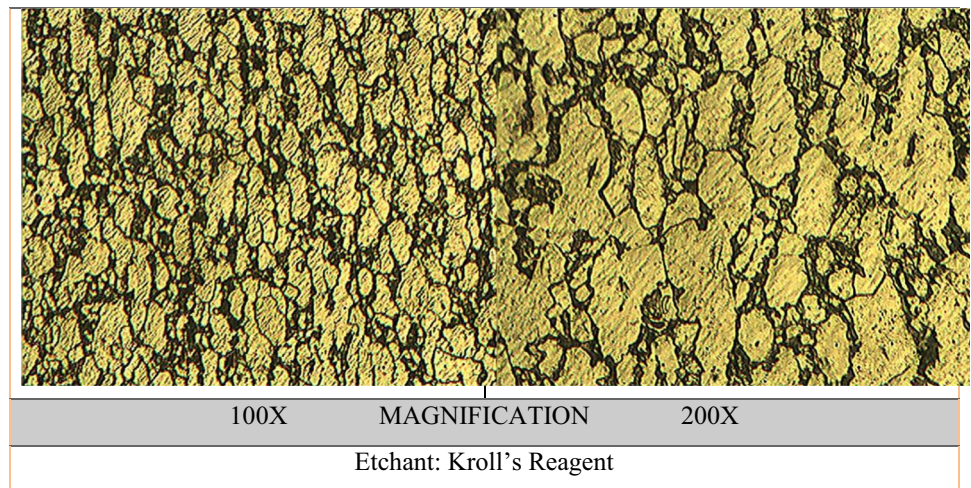
Thermal imaging camera (Model: FLIR-E63900, T198547) employed in the thermal image capturing can quantify the cutting temperature with brightness. The quantification of cutting temperature is done with respect to the reference temperature sourced by lamp. It can show the cutting temperature changes in colour variations. The camera estimates the cutting temperature at an accuracy of ±5 °C. The current setup of

**Table 1** Composition of Ti-6Al-4V alloy

Elements	Aluminum	Vanadium	Chromium	Copper	Iron	Manganese	Molybdenum	Niobium	Tin	Nickel	Silicon	Zirconium	Palladium	Carbon	Tungsten	Tantalum	Titanium
% By weight (%)	6.29	4.01	0.008	0.027	0.067	0.003	Less than 0.001	Less than 0.001	0.087	0.0043	0.0076	Less than 0.001	0.0122	0.097	Less than 0.025	0.0211	Remainder



**Fig. 2** Microstructure of titanium alloy (Ti64)



**Fig. 3** Experimental setup and thermal image capturing



measuring the thermal image complies with the safety standards ANSI B11.22-2002 (R2020). Prior to conducting the experiments, DoE was conducted with influencing independent parameters such as speed, feed and depth of cut. Table 3 reveals the range and levels selected for DoE ( $L_{16}$  orthogonal array). All experiments were conducted with PVD tool as well CVD carbide tool. No coolant (NC) was used in any experiment. The reason for dry machining is that the critical temperature at cutting can be investigated as NC does not take the advantage of coolant. Table 4 lists the cutting temperature generated at different cutting conditions, while the thermal images captured during experiments are presented and discussed in the next section. Figure 4 shows a turned Ti64 specimen with diameter of 85 mm and length of 125 mm.

## Results and Discussion

Turning of Ti64 samples were done with both CVD and PVD carbide tools according to  $L_{16}$  orthogonal matrix. The results listed in Table 4 shows the machinability of Ti64 alloy with CVD and PVD carbide inserts and the cutting temperature generated. Nevertheless, the temperature generated by CVD tool and PVD tool are not the same. Thermal images captured while machining the Ti64 alloy using PVD coated insert is shown in Fig. 5, while Fig. 6 shows the thermal images captured during machining of the same material using CVD coated insert.

Turning is the subtractive process where materials are removed as chips. Chips are characteristic evidence of the machining process. The built-up edge and tool wear can be estimated by analysing the chip formation. The size and form

**Table 2** Specification of CNC turning lathe being used in experiments

Make	PROTECK
Centre distance	2025 mm
Power of main motor	5.5kw
Spindle speed	100-3000 rpm
Length	1000 mm
Swing Diameter	450 mm

of chips vary according to the cutting condition. The chips collected during turning of Ti64 alloy using CVD and PVD coated carbide inserts are shown in Tables 5 and 6 respectively. As for as PVD coated carbide tool is concerned, long and continuous chips as well as short chips were witnessed. Continuous chip formation is due to high cutting temperature at the cutting zone. There is a shear localization observed, which is common in titanium machining. We could observe some undeformed materials also at the tip of chips. The temperature induced would affect the tool life and surface finish of the machined parts. Short chips were also appeared when temperature is lower. In contrast to the above, short chips were observed during the machining of Ti64 with CVD tool. Short chips do not form any adverse effect in machining titanium alloy.

For analysing the data, response surface methodology (RSM) is utilized. The regression analysis was done on the experimentally measured temperature data for two reasons. Firstly, to evaluate the performance of PVD and CVD coated inserts. Secondly to correlate the relationship between cutting parameters with cutting temperature.

$$T_{PVD} = 322.635 + 2.541v + 251.9f + 18d \tag{1}$$

$$T_{CVD} = 303.877 + 1.905v + 287.6f + 12.4d \tag{2}$$

Where as,  $T_{PVD}$  and  $T_{CVD}$  are temperatures (response parameters) in relation to PVD and CVD carbide inserts respectively.

Figure 7 compares the predicted result from  $T_{PVD}$  and experimental result, whereas Fig. 8 compares the predicted result from  $T_{CVD}$  and experimental result.

**Table 3** Levels used in DoE

Parameters	Range considered	Level 1	Level 2	Level 3	Level 4
Cutting Speed (v)	10 -70 m/min	10	30	50	70
Feed (f)	0.05 - 0.2	0.05	0.1	0.15	0.2
Depth of cut (d)	0.25 - 1.00	0.25	0.5	0.75	1.00

**Table 4**  $L_{16}$  Orthogonal array depicting cutting condition and cutting temperature measured from experiments (1 refers to Level 1, 2 refers to Level 2, 3 refers to Level 3 and 4 refers to Level 4)

Sl. No	Cutting Speed (m/min)	Feed (mm/rev)	Depth of cut (mm)	Temperature °C	
				PVD coated carbide insert	CVD coated carbide insert
1	1	1	1	344.4	323.3
2	1	2	2	353.3	344
3	1	3	3	405.8	394.6
4	1	4	4	413.3	397
5	2	1	2	454	397.2
6	2	2	1	455	406.9
7	2	3	4	466.6	417.5
8	2	4	3	467.4	414.9
9	3	1	3	475.4	425.2
10	3	2	4	487.8	427.9
11	3	3	1	486.5	443.7
12	3	4	2	507.3	462.3
13	4	1	4	524.8	460.7
14	4	2	3	533.2	480.7
15	4	3	2	544.6	489.3
16	4	4	1	553.8	495.4

The effectiveness of the RSM model was measured using root mean square values.  $R^2$  value and adjusted  $R^2$  value of  $T_{PVD}$  are 0.9516 and 0.9395 respectively.  $R^2$  value adjusted  $R^2$  value of  $T_{CVD}$  are 0.9412 and 0.9265 respectively. Both these models are significant with  $p < 0.05$ . Further to the analysis, RSM surface plots were drawn for both  $T_{PVD}$  and  $T_{CVD}$  models as shown in Figs. 9 and 10 respectively. Surface plots were drawn by holding one of the independent parameters constant and varying other two independent parameters. In both models, speed is noticed as a dominant parameter that effects the temperature rapidly. To this end, it is concluded



**Fig. 4** Turned Ti64 sample

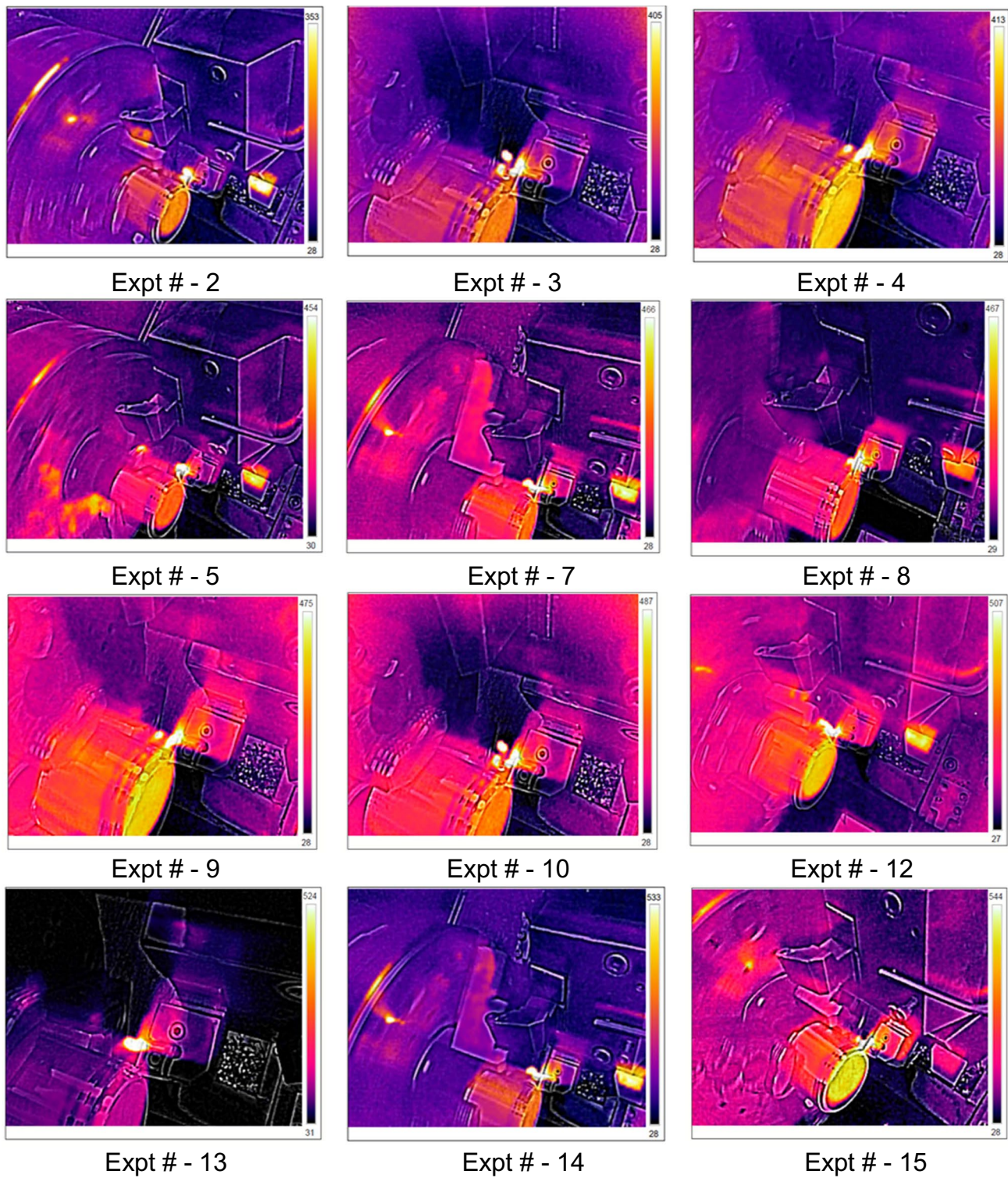


Fig. 5 Thermal images during machining of Ti64 alloy using PVD coated carbide insert

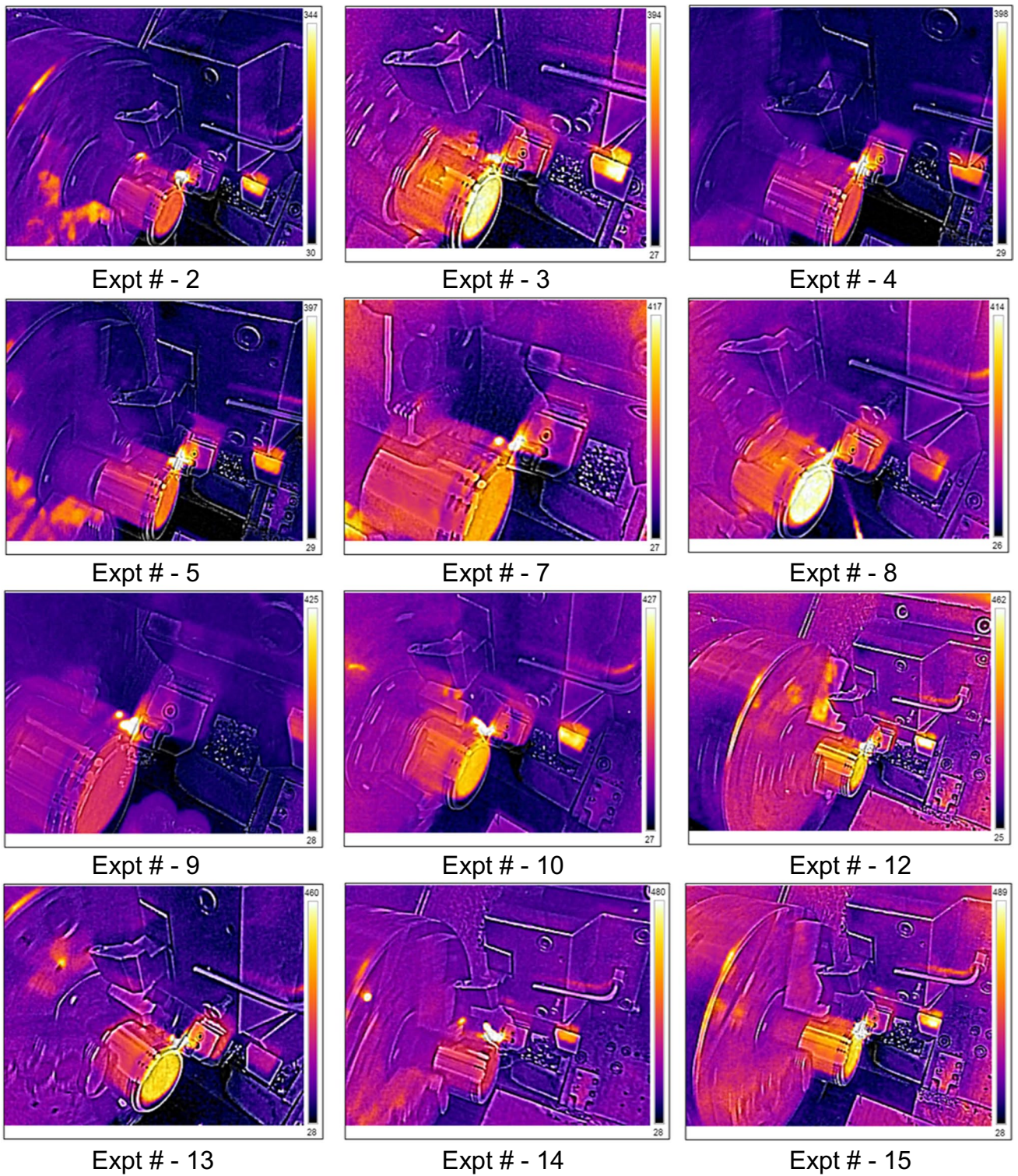
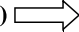





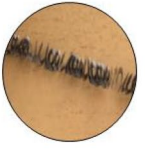













Fig. 6 Thermal images during machining of Ti64 alloy using CVD coated carbide insert

**Table 5** Chip formation while machining with CVD coated carbide insert

Feed (mm/rev) 	0.05	0.10	0.15	2
Cutting Speed (m/min) 				
10	 323°C	 344°C	 394°C	 397°C
30	 397°C	 406°C	 417°C	 414°C
50	 425°C	 427°C	 443°C	 462°C
70	 460°C	 480°C	 489°C	 495°C

**Table 6** Chip formation while machining with PVD coated carbide insert

Feed (mm/rev) 	0.05	0.10	0.15	2
Cutting Speed (m/min) 				
10	 344°C	 353°C	 405°C	 413°C
30	 454°C	 453°C	 466°C	 467°C
50	 475°C	 487°C	 486°C	 507°C
70	 524°C	 533°C	 544°C	 553°C



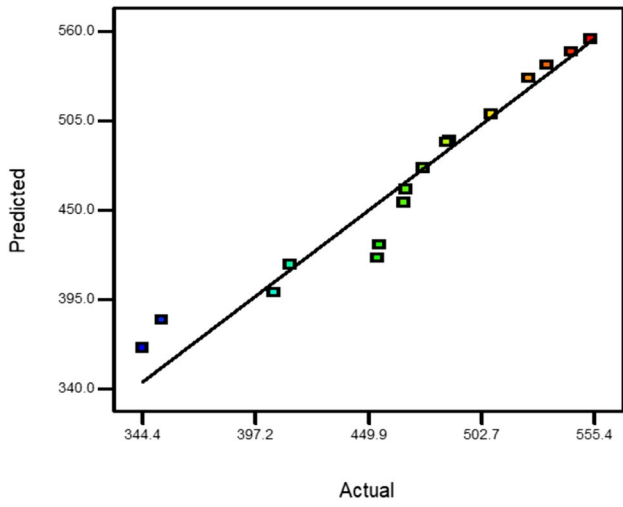


Fig. 7 Main effect plot between actual and predicted result from  $T_{PVD}$

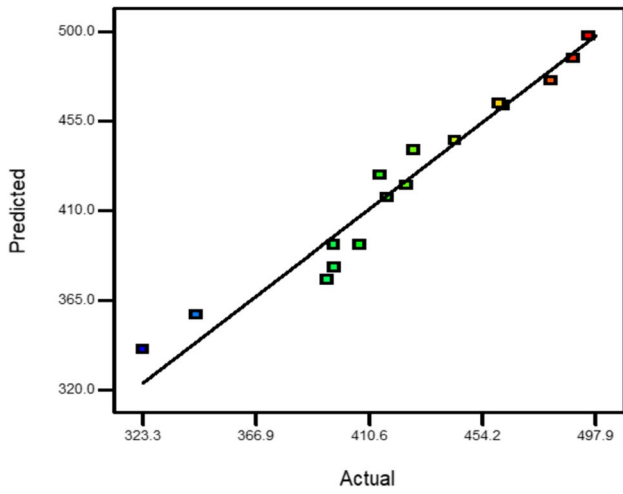


Fig. 8 Main effect plot between actual and predicted result from  $T_{CVD}$

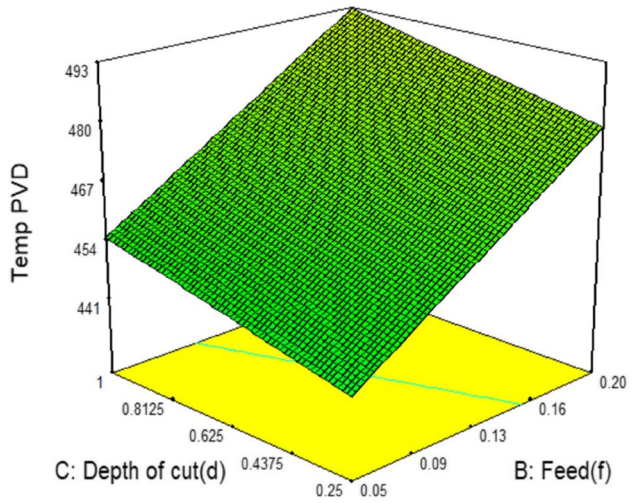
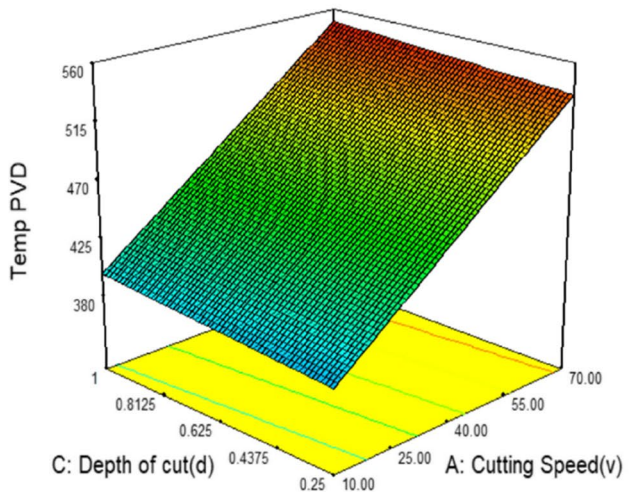
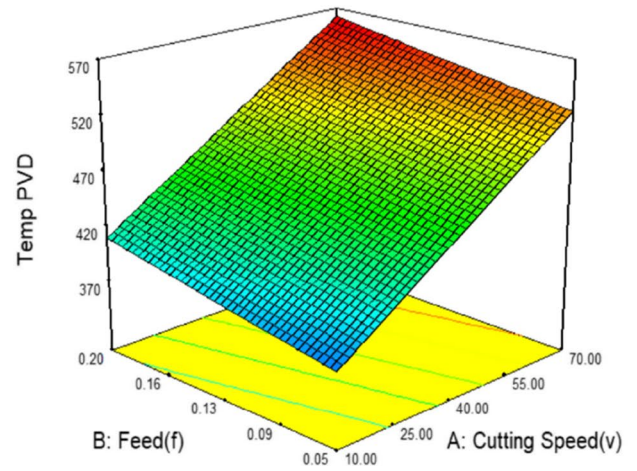


Fig. 9 Response surface plots of  $T_{PVD}$  model



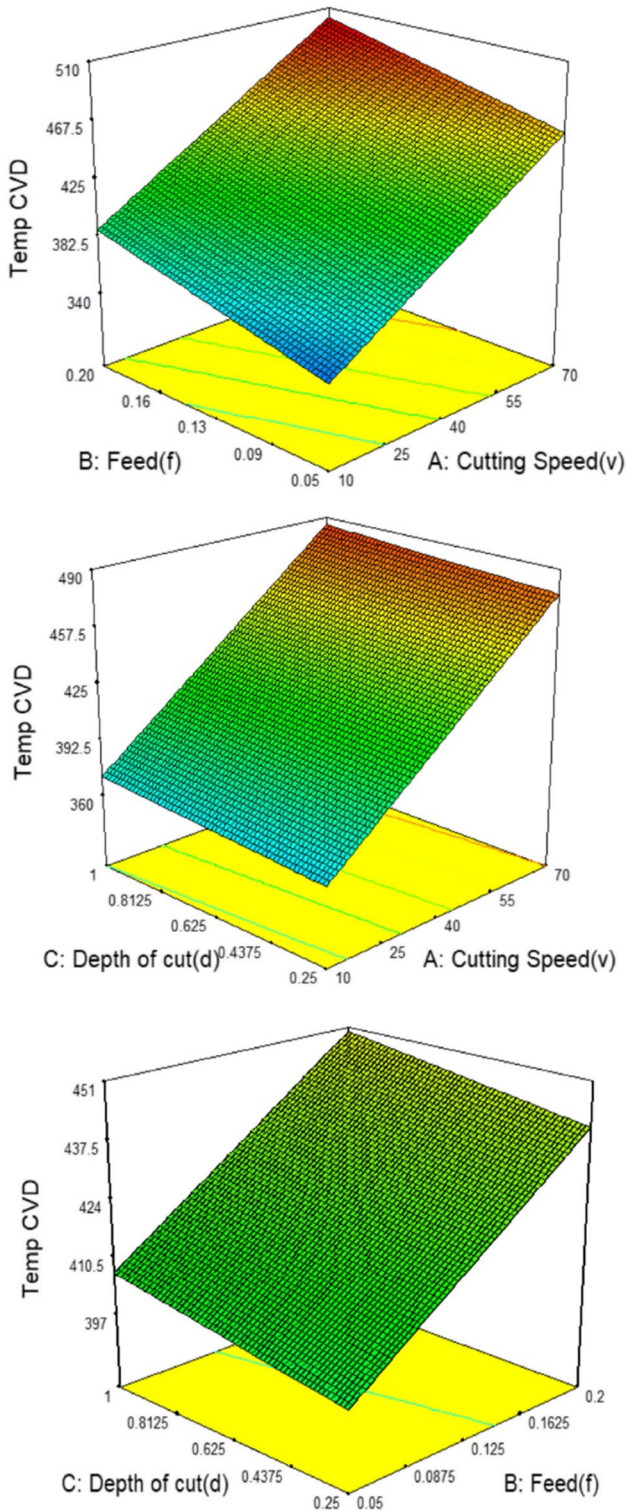


Fig. 10 Response surface plots of  $T_{CVD}$  model

that both tools are performing almost same in machining of titanium alloy, but comparatively PVD carbide tool is better than CVD carbide tool in machining Ti64 alloy.

Optimization of independent parameters for achieving the low cutting temperature was also attempted. Table 7 reveals the optimized parameters predicted by  $T_{CVD}$  model, while Fig. 11 depicts the thermal image captured during the validation experiments. It is noticed that the biasness of models is within acceptable limit (maximum error < 1.2%) (Fig. 11).

Table 8 shows  $T_{PVD}$  model predicted temperature and its respected independent parameters. Validation experiment was conducted, and thermal image was captured to measure the actual temperature for the same cutting condition (27 m/min, 0.10 mm/rev and 1.0 mm). Figure 12 shows the thermal image captured at the validation experiment. The actual temperature during machining and the predicted value is almost similar with  $\pm 1.6\%$  of error. It is concluded from this statistical analysis that both these models can be applied in machining of Ti64 alloy using PVD and CVD carbide tools.

### Conclusions

- Coated carbide inserts such as PVD and CVD were used for machining hard-to-machine material. Cutting speed is the prevailing parameter that effecting high cutting temperature. Feed rate and depth of cut have less effect on the cutting temperature as compared to speed.
- PVD and CVD carbide tools are used for machining Ti64 alloy, as they produces less temperature than HSS and other related tools.

Table 7 Optimized parameters for machining Ti64 alloy using CVD coated insert

$T_{PVD}$ predicted optimal cutting condition	Predicted Temperature (°C)	Actual Temperature measured from validation test (°C)	Error (%)
Cutting Speed (m/min)	30	396.85	±1.2%
Feed (mm/rev)	0.10	392.0	
Depth of cut (mm)	0.84	392.0	

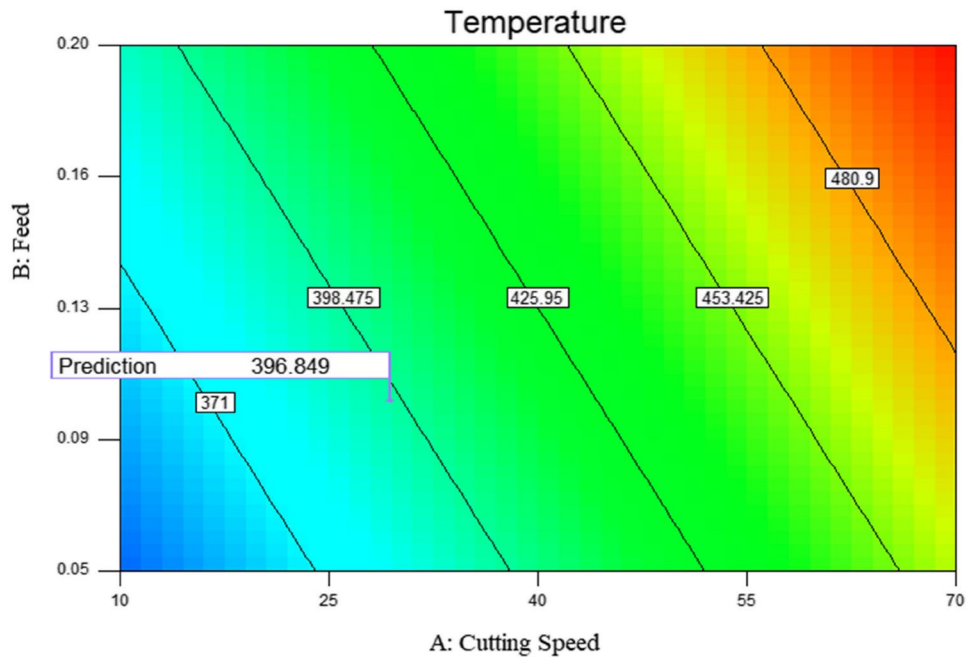


- The chips obtained for different temperatures are illustrated and presented in detail.
- Optimal cutting condition for machining Ti64 alloy was also predicted and validated experimentally. Predicted results have good agreement with experimental results.
- The temperature measured through this method gives only approximate value, the near-nett value can be obtained by using more sophisticated methods and tools.

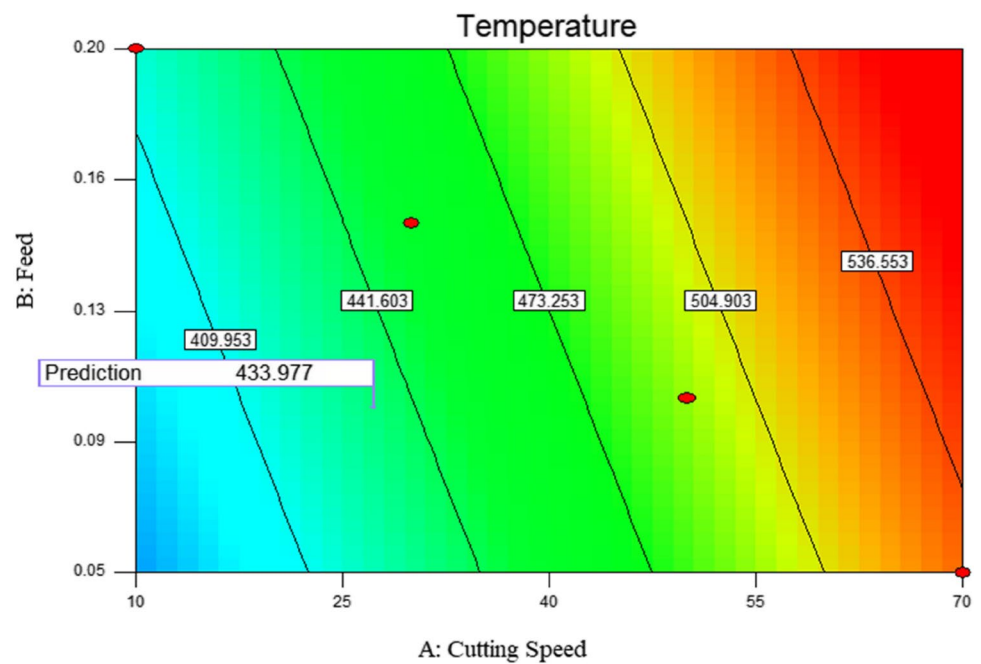
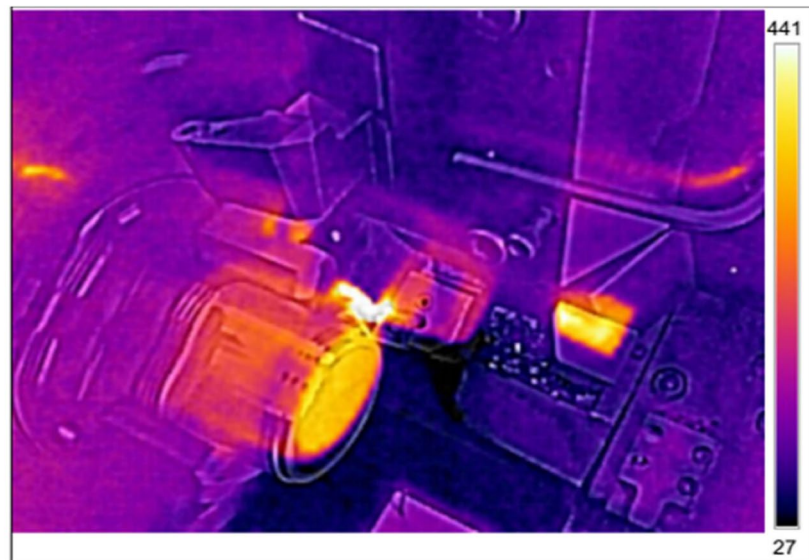
**Table 8** Optimized parameters for machining Ti64 alloy using PVD coated insert

$T_{CVD}$ predicted optimal cutting condition			Predicted Temperature (°C)	Actual Temperature measured from validation test (°C)	Error (%)
Cutting Speed (m/min)	Feed (mm/rev)	Depth of cut (mm)	433.97	441.0	±1.6%

**Fig. 11** Thermal image at optimized cutting condition using CVD coated carbide insert



**Fig. 12** Thermal image at optimized cutting condition using PVD coated carbide insert



## Declarations

**Conflict of Interest** The authors declare that there is no conflict of interest.

## References

1. Abhang LB, Hameedullah M (2010) Chip-tool interface temperature prediction model for turning process. *Int J Eng Sci Technol* 2(4):382–393
2. Gogia AK (2005) High temperature titanium alloys. *Defense Science Journal* 55(2):149–173
3. Donachie MJ (1988) *Titanium: a technical guide*, second edition. ASM international
4. Boyer RR (1996) An overview on the use of titanium in the aerospace industry. *Mater Sci Eng A* 213(1-2):103–114
5. Abukhshim NA, Mativenga PT, Sheikh MA (2006) Heat generation and temperature prediction in metal cutting: A review and implications for high-speed machining. *Int J Mach Tools Manuf* 46(7-8):782–800
6. Montgomery DC (1997) *Design and analysis experiments*, fourth edition. John Wiley & Sons Inc
7. Chomsamutr K, Jongprasithporn S (2012) Optimization parameters of tool life model using the Taguchi approach and response surface methodology. *Int J Comput Sci Issues* 9(1):120–125
8. Diniz AE, de Oliveira AJ (2004) Optimizing the use of dry cutting in rough turning steel operations. *Int J Mach Tools Manuf* 44(10):1061–1067

9. Ezugwu EO, Wang ZM (1997) Titanium alloys and their machinability—a review. *J Mater Process Technol* 68(3):262–274
10. Grzesik W, Nieslony P (2000) Thermal characterization of the chip-tool interface when using coated turning inserts. *J Manuf Process* 2(2):79–87
11. Ghani MU, Abukhshim NA, Sheikh MA (2008) An investigation of heat partition and tool wear in hard turning of H13 tool steel with CBN cutting tools. *Int J Adv Manuf Technol* 39:874–888
12. Hagqvist P, Sikström F, Christiansson A-K (2013) Emissivity estimation for high temperature radiation pyrometry on Ti–6Al–4V. *Measurement* 46(2):871–880
13. Heigel JC, Whinton E, Lane B, Donmez MA, Madhavan V, Moscoso-Kingsley W (2017) Infrared measurement of the temperature at the tool–chip interface while machining Ti–6Al–4V. *J Mater Process Technol* 243:123–130
14. Machado AR, Wallbank J (1990) Machining of titanium and its alloys—a review. *Proceedings of the Institution of Mechanical Engineers, Part B: Journal of Engineering Manufacture* 204(1):53–60
15. Muller B, Renz U, Hoppe S, Klocke F (2004) Radiation thermometry at a high-speed turning process. *J Manuf Sci Eng* 126(3):488–495
16. Müller-Hummel P, Lahres M (1995) Quantitative measurement of temperatures on diamond-coated tools during machining. *Diam Relat Mater* 4(10):1216–1221
17. Komanduri R, Von Turkovich BF (1981) New observation on the mechanism of chip formation when machining titanium alloys. *Wear* 69(2):179–188
18. Turley DM, Doyle ED, Ramalingam S (1982) Calculation of shear strains in chip formation in titanium. *Mater Sci Eng* 55(1):45–48
19. Narutaki N, Murakoshi A, Motonishi S, Takeyama H (1983) Study on machining of titanium alloys. *CIRP Annals* 32(1):65–69
20. Nithyanandam J, Das SL, Palanikumar K (2015) Influence of cutting parameters in machining of titanium alloy. *Indian J Sci Technol* 8(58):556–562
21. Rahman M, Wang ZG, Wong YS (2006) A review on high-speed machining of titanium alloys. *Journal Series C Mechanical Systems, Machine Elements and Manufacturing* 49(1):11–20
22. Ramesh S, Karunamoorthy L, Palanikumar K (2008) Surface roughness analysis in machining of titanium alloy. *Mater Manuf Process* 23(2):174–181
23. Ramesh S, Karunamoorthy L, Palanikumar K (2012) Measurement and analysis of surface roughness in turning of aerospace titanium alloy (gr5). *Measurement* 45(5):1266–1276
24. Viswanathan R, Ramesh S, Elango N, Kamesh Kumar D (2017) Temperature measurement and optimization in machining magnesium alloy using RSM and ANOVA. *Pertanika J Sci Technol* 25(1):255–262
25. Khanna N, Davim JP (2015) Design-of-experiments application in machining titanium alloys for aerospace structural components. *Measurement* 61:280–290
26. Kechagias JD, Aslani K-E, Fountas NA, Vaxevanidis NM, Manolakos DE (2020) A comparative investigation of Taguchi and full factorial design for machinability prediction in turning of a titanium alloy. *Measurement* 151:107213
27. Akkuş H, Yaka H (2021) Experimental and statistical investigation of the effect of cutting parameters on surface roughness, vibration and energy consumption in machining of titanium 6Al-4V ELI (grade 5) alloy. *Measurement* 167:108465
28. Aydın M, Karakuzu C, Uçar M, Cengiz A, Çavuşlu MA (2013) Prediction of surface roughness and cutting zone temperature in dry turning processes of AISI304 stainless steel using ANFIS with PSO learning. *Int J Adv Manuf Technol* 67(1):957–967
29. Aydın M, Köklü U (2020) Analysis of flat-end milling forces considering chip formation process in high-speed cutting of Ti6Al4V titanium alloy. *Simul Model Pract Theory* 100:102039
30. Aydın M (2021) Numerical study of chip formation and cutting force in high-speed machining of Ti-6Al-4V bases on finite element modeling with ductile fracture criterion. *Int J Mater Form*:1–14
31. Rajmohan T, Palanikumar K (2012) Optimization of machining parameters for surface roughness and burr height in drilling hybrid composites. *Mater Manuf Process* 27(3):320–328
32. Rajmohan T, Palanikumar K (2013) Modeling and analysis of performances in drilling hybrid metal matrix composites using D-optimal design. *Int J Adv Manuf Technol* 64:9–12
33. Srinivasan T, Palanikumar K, Rajagopal K, Latha B (2017) Optimization of delamination factor in drilling GFR–polypropylene composites. *Mater Manuf Process* 32(2):226–233

**Publisher's Note** Springer Nature remains neutral with regard to jurisdictional claims in published maps and institutional affiliations.

